antenna systems, etc. Taking into account the three-dimensionality of the antenna pattern will increase the accuracy of the orientation of additional means of protection against intentional interference, both in azimuth and on the angle of the place and more accurately solve the task of constructing an area of reach within which stable radio communication between power units is ensured. Software implementation of the proposed method allows to solve the problem of constructing a maximum zone of stable radio communication for a specific operational situation.

Keywords: *radio-electronic suppression, radio interference, radio communication channel, directional diagram.*

UDC: 531.383

V. Chikovani[1], H. Tsiruk[1], O. Korolova[2]

[1]*National Aviation University, Kyiv*
[2]*National Academy of Land Forces named after Hetman Petro Sakhajdachnyj, Lviv*

TRIPLE-MODE VIBRATORY GYROSCOPE

Coriolis vibratory gyroscope (CVG) is one of the chronologically latest gyroscopic technologies that appeared on the world market in the 90s of the last century. This technology has spread throughout the world for a relatively short time, mainly due to its micro-miniature version based on the micro-electro-mechanical system (MEMS), the so-called MEMS gyroscopes. There are two well-known modes of Coriolis vibratory gyro operation. These are rate mode and rate-integrating modes described in many works of different authors. There is also known dual mode CVG in which two abovementioned modes of operation have been combined in one gyro with automatic switching from one mode to another. Such a dual-mode CVG gains additional advantages over competing technologies, such as laser and fiber-optic gyroscopes. Recently, differential mode of operation for single mass CVG has been developed in Ukraine. It was shown that differential mode of operation has excellent external disturbances rejection properties.

This paper considers each mode of CVG operation and the questions of how to embed the differential mode into two first abovementioned ones to obtain triple-mode CVG which will widen application area and tighten position over competitive technologies. This triple-mode CVG can surely be realized in MEMS and non-MEMS gyros.

Thus, the following is defined, Differential CVG can be considered as third mode of operation for vibratory gyroscopes along with two well-known rate and rate-integrating ones. Differential mode of operation can be built-in the single gyro together with the two others, rate and rate-integrating modes, to implement triple-mode CVG. Triple-mode gyro can be implemented both for MEMS and non MEMS vibratory gyros.

Differential mode of operation has greater, than rate mode, external disturbances rejection factor and can be used when motion occurs in harsh environment.

Realization of triple mode CVG gives it highest «versatility» in comparison with competitive gyro technologies like ring laser gyro and fiber optic one.

Keywords: *Triple-mode CVG, MEMS gyro, rate mode, rate-integrating mode, differential mode.*

Introduction

Coriolis vibratory gyroscope (CVG) is one of the chronologically latest gyroscopic technologies that appeared on the world market in the 90s of the last century. This technology has spread throughout the world for a relatively short time, mainly due to its micro-miniature version based on the micro-electro-mechanical system (MEMS), the so-called MEMS gyroscopes.

There are two known modes of CVG operation: fist one is a force-rebalance mode, where Coriolis force arising due to rotation is compensated for by the negative feedback control system, holding the vibratory standing wave in a fixed position close to an excitation electrode, and hence, rotates together with a gyro. In this case the signal that compensates for the Coriolis force is proportional to angle rate. It is so-called rate mode of CVG operation. This mode of operation has been described in many works, for example [1–4].

The second mode is rate-integrating one, where Coriolis force is not compensated for. The quadrature signal is only compensated for to reduce measurement errors. In this mode of operation Coriolis force caused rotation of the vibratory standing wave relative to gyro and an angle of its rotation is proportional to an angle of a gyro rotation relative to the inertial space. Coefficient of proportionality between the angle of a gyro rotation relative to the inertial space and the angle of the standing wave rotation relative to gyro is called the

Bryan coefficient. This mode of operation has been described in many works, for example [1, 2, 5, 6].

The first and second modes of operation have been combined in dual-mode CVG [7].

Relatively recent investigations [8–10] conducted in Ukraine have led to the development of a third, differential, mode of CVG operation, which complements the first two modes. The differential mode of operation is realized by holding the standing wave between the electrodes by means of two excitation signals applied along two axes, located at the angle of 45^0 to each other. In this case, two measuring channels *X* and *Y* are formed, each of which provides a signal proportional to an angular rate with opposite signs +Ω and –Ω. The differential mode of operation has additional capabilities to compensate for the effects of both internal and external destabilizing factors when measuring angular rate [11, 12].

Problem statement

Analyze in detail each mode of operation, by representing a standing wave control system block diagram for each of them. Present and analyze standing wave control system block diagram combining all three modes in one gyro to realize a triple-mode CVG. Analyze advantages and disadvantages of each mode of operation. Based on this analysis propose an example of logic for automatic switching from one mode to another for triple-mode CVG. Graphically represent the results of simulations and measurements.

Rate mode CVG

CVGs fall into two classes, depending on the nature of the two vibratory modes involved. In the first class, the modes are different. An example of this class is the bar and tuning fork gyros, in which the mode driven is the ordinary vibration mode of the fork – primary mode, while the second or readout mode is the torsional oscillation of the fork about its axis of symmetry – secondary mode. The primary and secondary modes of bar and tuning fork gyros are depicted in fig. 1.

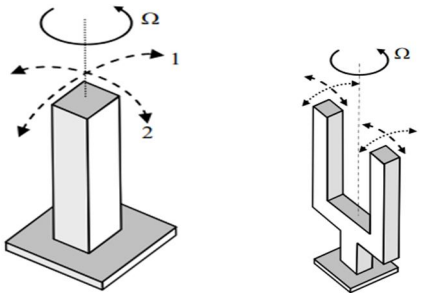

Fig. 1. **Resonators for the first class CVG**

In the second class, the two modes are identical, being two orthogonal modes (modes of the same natural frequency) of an axisymmetric elastic body. Examples are the vibrating cylindrical and hemispherical shells and ring, as depicted in fig. 2, and in fact any shell obtained as a body of rotation.

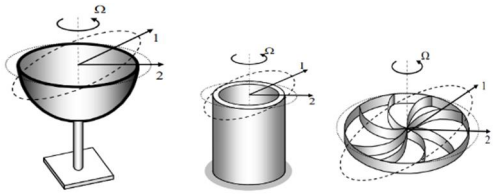

Fig. 2. **Resonators for the second class CVG**

The operation of a Coriolis vibratory gyroscope is based on sensitivity of elastic resonant structures to inertial rotation.

One of the most important parameters of resonators is quality factor (Q-factor), which depends on properties of a material from which the resonator is manufactured, and also on degree of an asymmetry of its shape etc. and is determined as:

$$Q = \omega_r \tau / 2 = \pi f_r \tau \,, \qquad (1)$$

where ω_r and f_r are circular and cyclic resonant frequency of a resonator, τ is a time of free oscillations amplitude damping *e* times.

In this paper we will focus on the second class CVG. Ring-type resonators shown in fig. 2 use the second mode of vibration to measure angle rate, because it has maximum sensitivity to rotation.

Fig. 3 shows the standing wave on the second resonant mode of the ring-type resonator which is characterized by 4 antinodes (maximum vibration amplitude) and 4 nodes (minimum vibration amplitude) located along circumferential coordinate under angles of 45 deg.

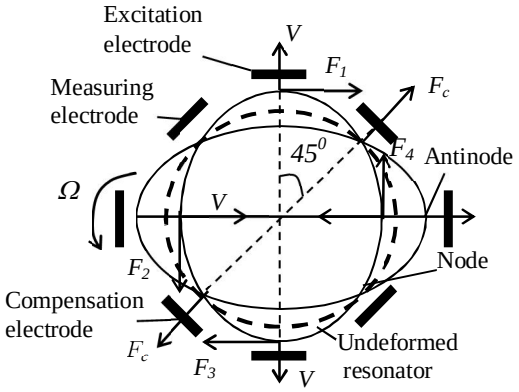

Fig. 3. **Standing wave in ring-type resonator**

Under resonator rotation with angle rate Ω, there arise Coriolis forces F_1, F_2, F_3, F_4 (fig.3), which generate secondary (Coriolis) mode of vibration in the direction of resultant force F_c.

Resultant Coriolis force is proportional to angle rate, Ω:

$$\vec{F}_c = 2m\left[\vec{\Omega} \times \vec{V}\right]; \qquad (2)$$

where V is a linear velocity of radial motion in process of vibration; m is an effective vibrating mass.

Thus, vibration amplitude generated by Coriolis force is proportional to angle rate Ω. Secondary (Coriolis) mode amplitude is measured by the electrode located at the node of the primary standing wave and with the aid of feedback control system is damped by applying compensation signal on the other node. Feedback control signal that compensates secondary mode of vibration is proportional to angle rate. Standing wave control system of the rate gyro is depicted in fig. 4.

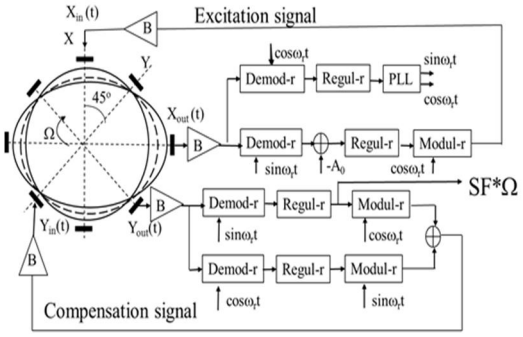

Fig. 4. **Rate CVG control system block diagram**

Diametrically opposite electrodes are connected between each other. As a result sensor has two input signals (X_{in}, Y_{in}) and two output signals (X_{out}, Y_{out}) (see fig. 4). It means that sensor can be considered as two-input-two-output plant. Vibration excitation is provided by supplying periodical signal to the X_{in} electrode at the resonant frequency. Response is picked off from the X_{out} electrode and it is used to sustain vibration and to track for changing of resonant frequency. Secondary mode amplitude is picked off from the Y_{out} electrode located at the nodal point of the primary wave and with the help of negative feedback signal is suppressed by supplying opposite phase signal to the Y_{in} electrode located at the other nodal point of the primary wave. Thus, feedback signal amplitude that compensates for the node vibration is proportional to angle rate Ω.

As has been shown in [1], after demodulation of signal from Y_{out} electrode using reference signal $\sin\omega_r t$, regulator generates compensation signal which is proportional to angle rate Ω. Coefficient of proportionality called scale factor (*SF*) and bias *B* as an error component can be determined as [1]:

$$\Omega = \frac{1}{SF} de\,\mathrm{mod}\{Y_{out}\}\big|_{\sin\omega_r t} + B; \qquad SF = 2k\omega_r A_0; \quad B = \frac{1}{2k}\Delta\left(\frac{1}{\tau}\right)\sin\theta_\tau. \tag{3}$$

Where A_0 is vibration amplitude, k is Brian coefficient determined by mode of vibration and resonator geometry, $\Delta(1/\tau)$ is a measure of resonator material non-homogeneity, θ_τ is a direction of maximum damping of resonator free oscillations. $\Delta(1/\tau)$ and θ_τ reduce to minimum by resonator mass-balancing procedure.

Fig. 5 shows rate CVG output signal, when rotating the gyro around vertical axis with its sensing axis is in horizontal plane. This curve is usually called azimuthal characteristic of the gyro. Average value of all measurements presented in fig. 5 is the gyro bias, which is about 25 deg/h. Maximum of the sine function shown in fig. 5 determines North direction, minimum – South direction, phase of this sine function determines azimuth of sensing axis initial position.

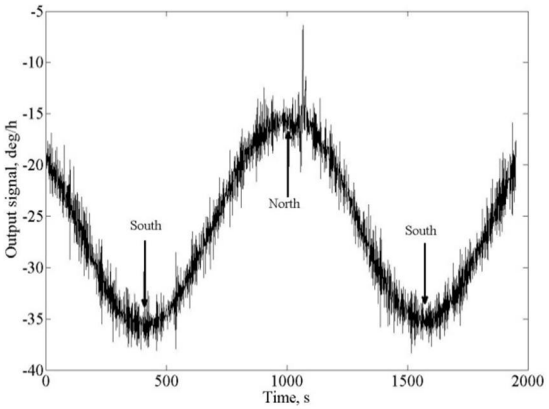

Fig. 5. **Rate CVG output signal when rotating sensing axis in horizontal plane**

Rate-Integrating mode CVG

Coriolis force caused by gyro rotation is not compensated for in the rate integrating mode of operation and as a consequence results in standing wave rotation through the angle proportional to gyro rotation angle relative to inertial space. Coefficient of proportionality between those two angles of rotation, i.e. rate integrating CVG scale factor, is called Brian coefficient k or angle gain coefficient.

$$\theta(t) = -k\alpha(t); \quad \alpha(t) = \int_0^t \Omega(\tau)\,d\tau; \tag{4}$$

where $\theta(t)$ is standing wave rotation angle with respect to a CVG; $\alpha(t)$ is a CVG rotation angle with respect to inertial space (distant stars).

In absence of gyro rotation resonator elementary mass point motion trajectory is ellipse shown in fig. 6.

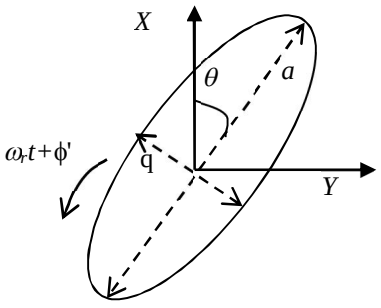

Fig. 6. **Mass point trajectory in oscillation.**

Ellipse parameters are designated as follows: a is vibration amplitude; q is quadrature amplitude; ω_r is

resonant frequency; ϕ' is vibration phase; θ is vibrating pattern orientation relative to *X* axis (drive electrode).

At a gyro rotation the ellipse turns with the lag coefficient *k*. For cylinder resonator Brian coefficient *k* can be calculated using expression [13]:

$$k = \frac{n}{n^2 + 1 + \frac{3}{n^2}\left(\frac{r}{h}\right)^2}, \quad (5)$$

where *n* is a number of vibration mode (*n*=2); *r* is a cylinder radius; *h* is a cylinder height.

For example, for cylinder size: *r*=6 mm and *h*=10 mm, *k*≈0.38, so, if CVG rotation angle relative to inertial space is 90^0, standing wave rotation angle relative to CVG is $\theta=-0.38*90=-34.2^0$. For bar resonator, shown in fig.1, Brian coefficient for the first mode is *k*≈1 [3]. This means that a standing wave is almost immovable relative to inertial space and is a zero reading for CVG inertial rotation angle measurement.

Frequency mismatch Δ*F* and *Q*-factor mismatch Δ*Q* resulting from resonator manufacturing imperfections and external forces result in that parameters *a*, *q*, ϕ' and θ are changing versus time. They are changing much slower than vibration period $T=2\pi/\omega_r$. In order to calculate parameters *a*, *q*, ϕ' and θ, demodulation should be used based on mixing the signals $X_{out}(t)$ and $Y_{out}(t)$ with reference signals $\sin\omega_r t$ and $\cos\omega_r t$ and low pass filtering to obtain four demodulated variables C_x, S_x, C_y, S_y as shown in fig. 7.

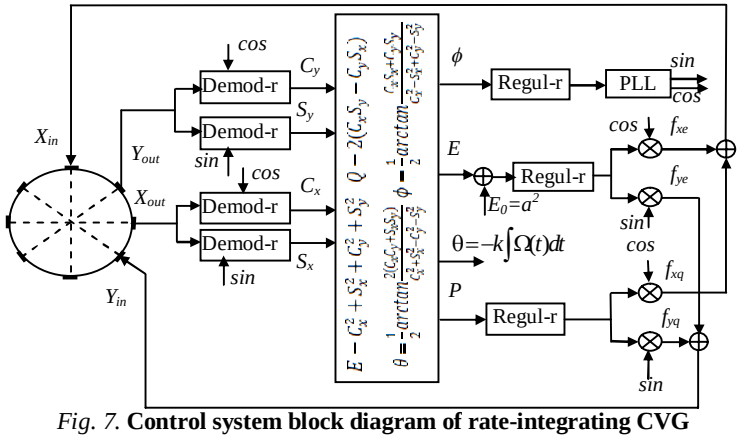

Fig. 7. **Control system block diagram of rate-integrating CVG**

Parameters *a*, *q*, ϕ' and θ are calculated by the following expressions [14]:

$$a=\sqrt{\frac{1}{2}\left(E+\sqrt{E^2-P^2}\right)};\ q=\sqrt{\frac{1}{2}\left(E-\sqrt{E^2-P^2}\right)};$$
$$E=C_x^2+S_x^2+C_y^2+S_y^2;\quad P=2(C_xS_y-C_yS_x); \quad (6)$$
$$\theta=\frac{1}{2}\arctan\frac{2(C_xC_y+S_xS_y)}{C_x^2+S_x^2-C_y^2-S_y^2};\ \phi'=\frac{1}{2}\arctan\frac{2(C_xS_x+C_yS_y)}{C_x^2-S_x^2+C_y^2-S_y^2};$$

The aim of the CVG control system in rate integrating mode of operation is to keep the standing wave parameters in process of operation at the following values:

$$P=0\rightarrow q=0,\ a^2=E=const,\ \phi=0; \quad (7)$$

Fig. 8 shows mass point trajectories when *q*≈*0* and *q*≠*0* during standing wave rotation.

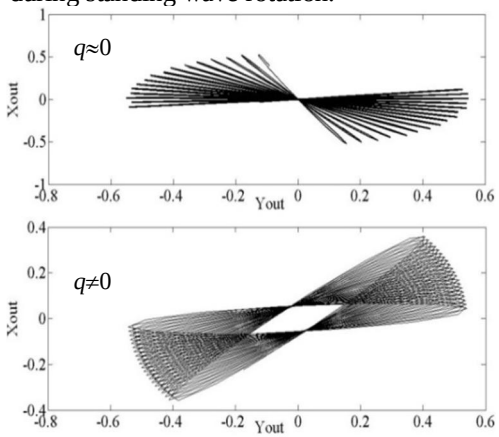

Fig. 8. **Mass point trajectory when q≈0 and q≠0**

The upper graph presents oscillation along straight line and rotation counter-clock-wise, when quadrature component is compensated for q≈0. The lower graph presents oscillation trajectory along ellipse with quadrature component q≠0.

Fig. 9 shows measurement of 10 Hz periodic input rotation angle by CVG with the following resonator's imperfections Δ*Q*/*Q*=5% and Δ*F* =0.1 Hz and internal electronics noise equal to σ_{noise}=0.089 rad. As can be seen from fig. 9, it is expedient to have more perfect resonator to measure rotation angle in rate-integrating mode of operation. Rate-integrating CVG has higher sensitivity to resonator imperfections, than rate mode and differential mode. However, scale factor of rate integrating CVG is a very stable constant that gives small dynamic error when measuring high angle rate.

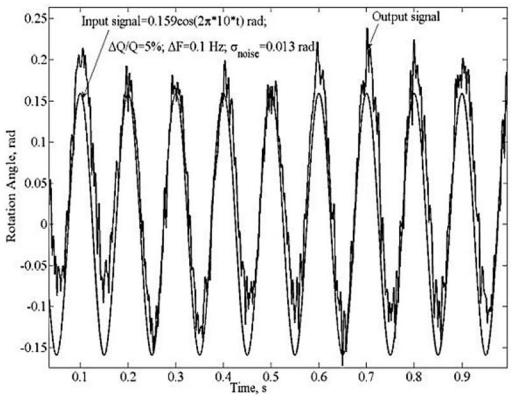

Fig. 9. **Measurement of periodic input rotation angle by rate-integrating CVG**

Differential Mode CVG

In differential CVG standing wave is located between the electrodes so that wave angle $\theta \neq m\pi/4$, $m=0, 1\ldots$, that is standing wave oscillation direction is not coincident with any of the electrodes. In this case measurement equations can be written as [12]:

$$\begin{aligned} -2k\Omega D_y \sin 2\theta + D_x d_{xx} \cos\theta + d_{xy} D_y \sin 2\theta = z_x; \\ 2k\Omega D_x \cos 2\theta + D_y d_{yy} \sin\theta + d_{xy} D_x \cos 2\theta = z_y, \end{aligned} \quad (8)$$

where

$$d_{xx} = \left[\frac{2}{\tau} + h\cos 2(\theta - \theta_\tau)\right]; \; h = \Delta\left(\frac{1}{\tau}\right) = \frac{1}{\tau_1} - \frac{1}{\tau_2};$$

$$\frac{2}{\tau} = \frac{1}{\tau_1} + \frac{1}{\tau_2}; \; d_{yy} = \left[\frac{2}{\tau} - h\cos 2(\theta - \theta_\tau)\right];$$

$$d_{xy} = h\sin 2(\theta - \theta_\tau).$$

D_x and D_y are transformation coefficients of deformations into voltages by the X and Y electrodes.

As can be seen from the first equation of (8) angle rate Ω has negative sign, and in the second one it has positive sign. Thus, control system that holds standing wave between electrodes realizes differential mode of operation for CVG.

To effectively realize differential mode of operation it is necessary to align standing wave under angle θ^* at which the following condition is valid:

$$\begin{aligned} 2kD_y \sin 2\theta^* = 2kD_x \cos 2\theta^*; \\ \theta^* = \frac{1}{2} a\tan\frac{D_x}{D_y} = \frac{1}{2} a\tan\left(\frac{SF_y^\theta}{SF_x^\theta}\tan 2\theta\right), \end{aligned} \quad (9)$$

where SF_x^θ and SF_y^θ are X and Y channel scale factors at standing wave angle θ.

When standing wave angle is θ^*, the difference, z_y-z_x, of two X and Y channel measurement signals are:

$$z_y - z_x = SF_d\left(\Omega + \frac{d_{yy} - d_{xx}}{4k}\right); \quad (10)$$

where SF_d is a scale factor of differential CVG when standing wave angle $\theta = \theta^*$.

$$SF_d = 4k\frac{D_x D_y}{\sqrt{D_x^2 + D_y^2}}. \quad (11)$$

As can be seen form (10) the differential CVG output signal does not contain damping cross-coupling d_{xy}. This error is compensated for by subtracting two channels measurements.

Differential CVG control system block diagram is presented in fig. 10.

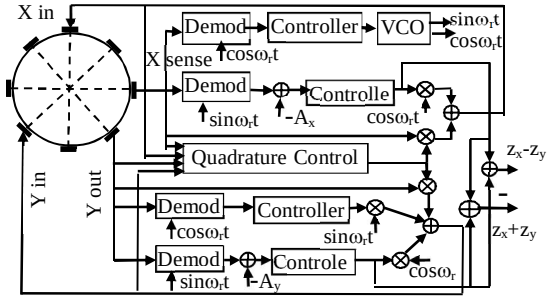

Fig. 10. **Differential CVG control system block diagram**

Due to the equality of the scale factors of the two measuring channels, the external disturbances affecting the gyroscope have the same response and when the signals are subtracted they are compensated for zero. However, with strong external disturbances, nonlinear components appear in the output signals, which are partially compensated and lead to residual uncompensated errors.

It was experimentally shown in [12] that for such disturbances as acoustic impulse, a constant and alternating magnetic field the rejection factors reach high levels (no less than 65).

For small shocks differential CVG shock rejection factor as shown in fig.11 is large enough. As can be from fig. 11 half difference of X and Y channels are close to zero. It means that small shocks contribute equal errors to two channels and they are subtracted.

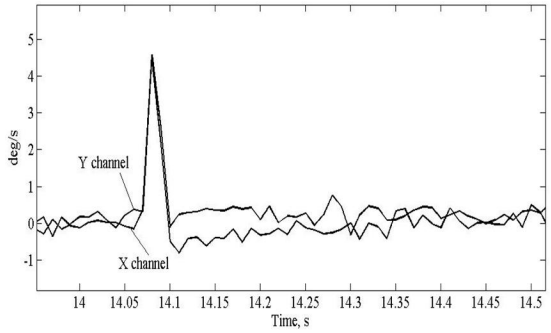

Fig. 11. **Differential CVG responses to small shock along input axis**

However, for high level shocks (100 g) asymmetric distortions of the gyro's structural elements reduce the shock rejection factor. As can be seen from fig. 12 shock rejection factor is about 3. Analyzing results presented in figs.11 and 12 and taking into account more detailed test results presented in [11, 12] one can conclude that differential mode of operation has greater, than rate mode, external disturbance rejection factor and less sensitivity to the following disturbances like shocks, vibrations, acoustic impulses and magnetic fields.

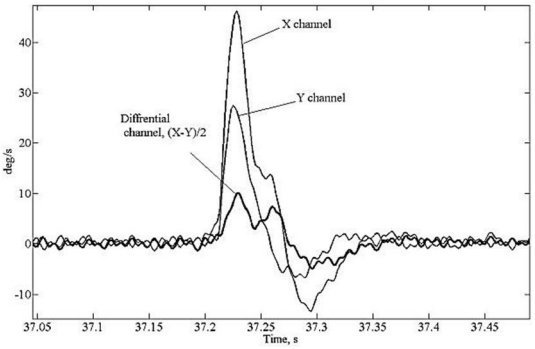

Fig. 12. **Differential CVG responses to 100 *g* shock along input axis**

Triple mode CVG

CVG differs from other modern gyros – ring laser and fiber optic - by that all three considered in this paper mode of operations can be realized in one CVG to

provide accuracy requirements for different motion and environmental conditions. For example, under measuring of small angle rate it is advisable to operate in the rate mode, since the measurement errors are mainly determined by noise and bias drift which can be lower, than that of rate-integrating modes of operation. Under measuring of high angle rate, it is advisable to operate in the rate-integrating mode of operation since the measurement errors in this mode are mainly determined by multiplicative error $\Delta\Omega$ caused by scale factor uncertainty (ΔSF), $\Delta\Omega=\Delta SF\cdot\Omega$. Scale factor for rate-integrating mode of operation is a stable constant (Bryan coefficient). It can reach 35 ppm and its dynamic range can reach $7\cdot10^3$ deg/s even for low-cost gyros [15].

Triple mode CVG can be realized for MEMS and non-MEMS CVG on the basis of modified rate-integrating algorithm, presented in fig. 7, with ability to automatically switch from one mode to another.

Block diagram of triple mode CVG is presented in fig. 13. This block diagram uses switcher 1 to switch from one mode to another.

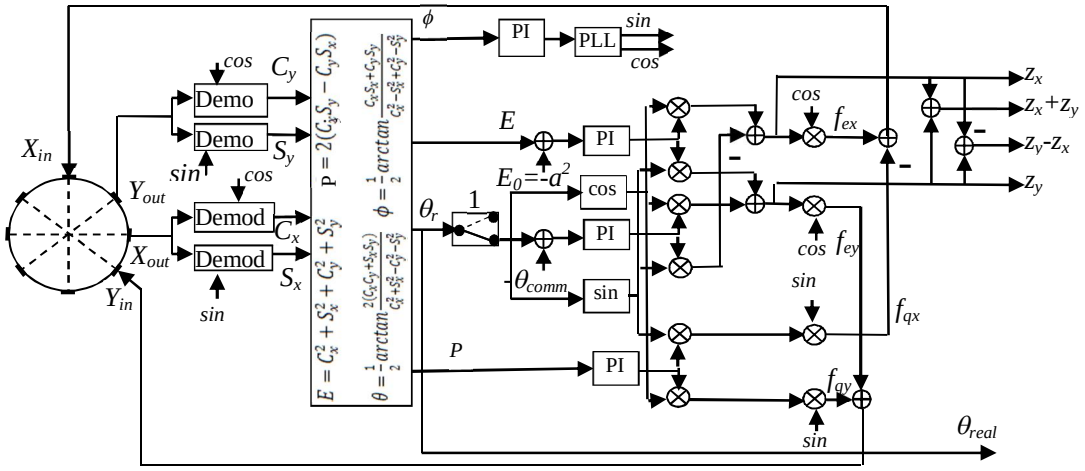

Fig. 13. **Triple mode CVG control system block diagram**

When switcher 1 is in the position shown in fig. 13 and command angle θ_{comm} is fixed at one of the values from a set of $\theta_{comm}=m\pi/4$, m=0, 1, 2…, it operates in rate mode. When command angle θ_{comm} is fixed at one of the values from a set of $\theta_{comm}\neq m\pi/4$, it operates in differential mode and when switcher 1 is open (dashed line in fig. 13) it operates in rate integrating mode.

Fig. 14 shows three modes of CVG operation with automatically switching from one mode to another.

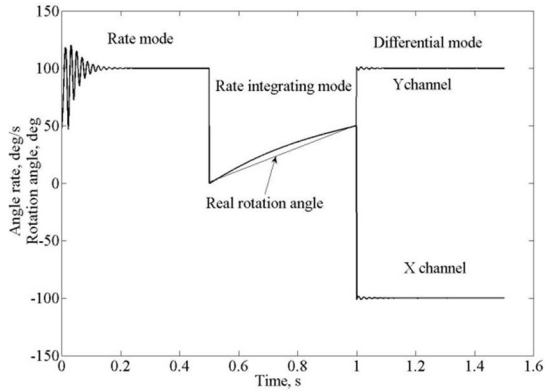

Fig. 14. **Triple mode CVG measurements**

First mode is a rate one that measures angle rate of 100 deg/s, then it is switched to rate integrating mode without changing angle rate. Deviation from straight line in this mode of operation is due to resonator manufacturing imperfections. Then it is switched to differential mode of operation with two output signals 100 deg/s and -100 deg/s. Difference of these signals has the ability to compensate for the errors due to external disturbances. Sum of these signals can also be used to estimate residual errors.

In order to realize triple mode CVG with modes switching, advantages and disadvantage of each mode of operation should be analyzed.

Advantages and disadvantages of three modes of operations are presented in the table 1.

Table 1

Advantages and disadvantages of CVG modes of operation

Rate CVG	Rate Integrating CVG	Differential CVG
Advantages		
• Low noise • Standing wave control simplicity • Easy to calibrate resonator's imperfections	• High dynamic range • High bandwidth • High stability of scale factor	• Higher resistivity to external disturbances • Effective on-line compensation for the frequency mismatch • Possibility to on-line bias compensation
Disadvantages		
• Higher sensitivity to external disturbances • Lower scale factor temperature stability • Limited bandwidth	• Higher sensitivity to resonator's imperfections • Higher noise especially when measuring small angle rate	• Limited bandwidth • Lower scale factor temperature stability

Based on the results of the above table switching logic presented in fig. 15 can be proposed.

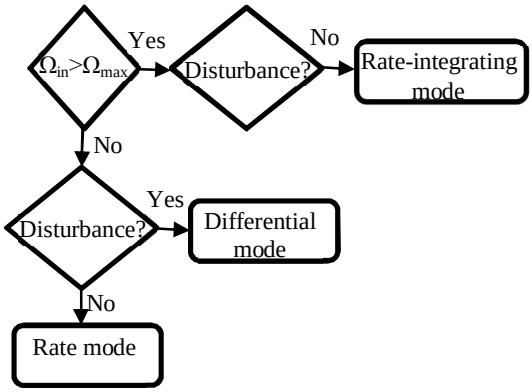

Fig. 15. **Example of modes switching logic**

This switching logic is based on one criterion if Ω_{input} is more than Ω_{max} which is determined from practical considerations the rate-integrating mode of operation should be used. However, in case of presence of external disturbances differential mode of operation should be chosen. In all other cases rate mode should be chosen. Other more complex logic can be developed for different practical applications based on advantages and disadvantages of modes of CVG operation.

Conclusion

Differential CVG can be considered as third mode of operation for vibratory gyroscopes along with two well-known rate and rate-integrating ones. Differential mode of operation can be built-in the single gyro together with the two others, rate and rate-integrating modes, to implement triple-mode CVG. Triple-mode gyro can be implemented both for MEMS and non MEMS vibratory gyros.

Differential mode of operation has greater, than rate mode, external disturbances rejection factor and can be used when motion occurs in harsh environment.

Realization of triple mode CVG gives it highest «versatility» in comparison with competitive gyro technologies like ring laser gyro and fiber optic one.

References

1. Lynch D.D.: Coriolis Vibratory Gyroscope, IEEE Standard Specification Format Guide and Test Procedure for Coriolis Vibratory Gyros, IEEE std.1431TM, Annex B, pp. 56-66, Dec. 2004.

2. Gregory J.A.: Characterization Control and Compensation of MEMS Rate- and Rate-Integrating Gyroscopes». – Ph.D. Dissertation, Michigan University, P. 198, 2012.

3. Cho J.Y.: High-Performance Micromachined Vibratory Rate- And Rate- Integrating Gyroscopes, Ph.D. Dissertation, Michigan University, P. 293, 2012.

4. Zhong Su, Ning Liu, Qing Li, Mengyin Fu, Hong Liu, Junfang Fan: Research on the Signal Process of a Bell-Shaped Vibratory Angular Rate Gyro, Sensors, 14, 5254-5277, 2014; doi: 10.3390/s140305254.

5. Gallacher B., Hu Zh., Bowles S.: Full control and compensation scheme for a rate-integrating MEMS gyroscope, 13th Int. Conf. on Dynamical Systems – Theory And Applications, Lodz, Poland, paper id: ENG267, Dec. 7–10, 2015.

6. Woo J-K., Cho J.Y., Boyd Ch., Najafi Kh.: Whole-Angle-Mode Micromachined Fused-Silica Birdbath Resonator Gyroscope (Wa-Brg), IEEE MEMS Conf., San Francisco, CA, USA, January 26–30, 2014.

7. Lynch D.D., Matthews A.: Dual Mode Hemispherical Resonator Gyro Operating Characteristics, 3-rd S. Petersburg Int. Conf. on Integrated Navigation Systems, part 1, pp. 37–44, May 1996.

8. Chikovani V.V., Umakhanov E.O., Marusyk P.I.: The compensated differential CVG, Gyro Technology Symposium, Germany, Karlsruhe university, pp. 31-38, 16-17 Sept. 2008.

9. Чіковані В.В. Спосіб виміру кутової швидкості коріолісовим вібраційним гіроскопом. – Пат. 95709, Україна, МПК G01 C 19/02. – Опубл. 25.08.2011, бюл. № 16/2011.

10. Chikovani V.V., Suschenko O.A. Differential mode of operation for ring-like resonator CVG, IEEE Proc. Intern. Conf. on Electronics and Nanotechnology, Kyiv, Ukraine, pp. 451–455, 15–18 April 2014.

11. Valerii V. Chikovani, Olha A. Sushchenko, Hanna V. Tsiruk «External Disturbances Rejection by Differential Single-Mass Vibratory Gyroscope». – Acta Polytechnica Hungarica, 2017, vol. 14, № 3, pp. 251-270.

12. Chikovani V.V., Tsiruk H.V. Effective Rejection Of Acoustic And Magnetic Field's Disturbances By Single-Mass Differential Vibratory Gyroscope. – Військово-технічний Збірник, Національна академія сухопутних військ ім. П. Сагайдачного, Львів. – № 16. – 2017. – С. 31–37.

13. Матвеев В.А., Лунин Б.С., Басараб М.А. Навигационные системы на волновых твердотельных гироскопах. – М.: Физматлит, 2008. – С. 240.

14. Lynch D. Vibratory Gyro Analysis by the Method of Averaging, Proc. 2nd St. Petersburg Conf. on Gyroscopic Technology and Navigation, St. Petersburg, Russia, May 24-25, 1995, pp. 26–34.

15. Jeanroy A., Featonby P., Caron J-M.: Low-Cost Miniature and Accurate Sensors for Tactical Applications, 10-th S. Petersburg Int. Conf. on Integrated Navigation Systems, pp. 286–293, May, 2003.

Рецензент: д.т.н., проф. В.М. Азарсков, Національний авіаційний університет, Київ.

ТРИРЕЖИМНИЙ ВІБРАЦІЙНИЙ ГІРОСКОП

В.В. Чіковані, Г.В. Цірук, О.В. Корольова

Є два відомі режими роботи коріолісового вібраційного гіроскопа (КВГ). Це режим датчика кутової швидкості та режим інтегруючого гіроскопа, що описані в багатьох роботах різних авторів. Існує також відомий дворежимний КВГ, в якому два вищевказані режими роботи були об'єднані в одному гіроскопі з автоматичним переключенням від одного режиму до іншого. Такий дворежимний КВГ отримує додаткові переваги над конкуруючими технологіями, такими як лазерні та волоконно-оптичні гіроскопи. Режими роботи можуть змінюватися в залежності від значення

кутової швидкості або зовнішніх умов для забезпечення максимальної точності вимірювань. Недавно в Україні розроблено диференційний режим роботи КВГ. Показано, що диференційний режим роботи має відмінні властивості придушення зовнішніх збурень. У даній роботі розглядається кожен режим роботи КВГ та як вбудувати диференціальний режим у два перших вищезазначених режими, для одержання трирежимного КВГ, який розширить галузь застосування та посилить переваги над конкурентними технологіями. Цей трирежимний КВГ можна безперечно реалізувати як на основі мікромеханічного, так і немікромеханічного КВГ.

Ключові слова: *трирежимний КВГ, МЕМС гіроскоп, режим кутової швидкості, інтегруючий режим, диференційний режим.*

ТРЕХРЕЖИМНЫЙ ВИБРАЦИОННЫЙ ГИРОСКОП

В.В. Чиковани, Г.В. Цирук, О.В. Королёва

Есть два известных режима работы кориолисового вибрационного гироскопа (КВГ). Это режим датчика угловой скорости и режим интегрирующего гироскопа, которые описаны во многих работах разных авторов. Существует также известный двухрежимный КВГ, в котором два вышеуказанных режима работы объединены в одном гироскопе с автоматическим переключением с одного режима на другой. Такой двухрежимный КВГ получает дополнительные преимущества над конкурирующими технологиями, такими как лазерные и волоконно-оптические гироскопы. Режимы работы могут меняться в зависимости от значения угловой скорости или внешних условий для обеспечения максимальной точности измерений. Недавно в Украине разработан дифференциальный режим работы КВГ. Показано, что дифференциальный режим работы имеет отличные свойства подавления внешних возмущений. В данной работе рассматривается каждый режим работы КВГ и как встроить дифференциальный режим в два первых вышеупомянутых режима, для получения трехрежимного КВГ, который расширит область применения и усилит преимущества над конкурентными технологиями. Этот трехрежимный КВГ можно бесспорно реализовать как на основе микромеханического, так и немикромеханического КВГ.

Ключевые слова: *трехрежимный КВГ, МЕМС гироскоп, режим угловой скорости, интегрирующий режим, дифференциальный режим.*